Systems & Control Transactions

**Original Research Article**
*Peer Reviewed Conference Proceeding*
ESCAPE 36 - European Symposium on Computer Aided Process Engineering
Sheffield, UK. 21-24 June 2026

PSE PRESS

# Modeling, Simulation, and Optimization of an Anion Exchange Membrane Cell for Ammonia Electrolysis

**Laureen E. Hernández Lefrán, Leonardo A. Cáceres Avilez, Antonio E. Bresciani, Claudio A. Oller do Nascimento, Rita M. Brito Alves***

Universidade de São Paulo, Escola Politécnica, Department of Chemical Engineering, São Paulo, São Paulo, Brazil
* Corresponding Author: rmbalves@usp.br

## ABSTRACT

The need to reduce greenhouse gas emissions and diversify energy sources has driven the development of hydrogen ($H_2$) as a leading carbon-free energy vector with high gravimetric energy density (33.3 kWh/kg) for stationary and transport applications. However, its storage and transportation remain challenging. Therefore, ammonia emerges as a promising hydrogen carrier due to its high energy density and ease of liquefaction and transport. This work presents the development of a phenomenological based mathematical model for an ammonia electrolysis cell operating in a zero-gap configuration with an anion exchange membrane. The model considers the contributions of different overpotentials (activation, ohmic, concentration) and incorporates empirical and semi-phenomenological expressions adjusted to experimental data from Zhang et al [1]. The model shows both qualitative and quantitative agreement with experimental measurements, achieving a determination coefficient ($R^2$) of 0.9874. Beyond electrochemical modeling, the cell model is integrated into a nonlinear programming (NLP) optimization framework to minimize the total annualized cost (TAC) of the system. For hydrogen production of 1250 kg/h, the optimal solution corresponds to 353 K, 0.82 A/cm$^2$, and 1302 cells, yielding a TAC of about 45.0 MUSD/year.

**Keywords**: Hydrogen production, Ammonia electrolysis, Zero gap cell, Mathematical model, Optimization

## INTRODUCTION

Hydrogen ($H_2$) is widely regarded as a promising energy vector due to its high gravimetric energy density and carbon-free end use [2]. However, its low volumetric energy density and wide flammability range pose challenges for storage and long-distance transportation, requiring energy-intensive solutions such as high-pressure compression or cryogenic liquefaction [2-3].

A promising alternative to overcome these limitations involves storing hydrogen in chemical compounds that can be easily transported and stored, with hydrogen released on demand through chemical or electrochemical processes. Among the available hydrogen carriers, ammonia ($NH_3$) stands out due to its high hydrogen content (17 wt.%), relatively mild liquefaction conditions (~10 bar at ambient temperature), and well-established global infrastructure [4-5].

In this context, ammonia electrolysis has emerged as an attractive pathway for hydrogen production, offering a significant thermodynamic advantage over conventional water electrolysis [5]. Recent studies highlight that anion exchange membrane (AEM) electrolyzers are particularly suitable for ammonia electrolysis due to their chemical compatibility with $NH_3$ and their ability to operate under alkaline conditions. Furthermore, zero-gap cell configurations have been identified as the most promising architecture, as they minimize internal ohmic losses while enabling compact and scalable designs for industrial deployment [6]. However, despite the growing number of experimental studies, the availability of mathematical models for system-level analysis and scale-up remains limited.

The present work addresses this gap by developing a mathematical model of an anion exchange membrane ammonia electrolyzer within a compact zero-gap configuration.

The Methods section describes the electrolyzer configuration, the modeling approach and assumptions, the parameter estimation procedure, and the formulation

of the optimization problem, minimizing the total annualized cost (TAC). The model was parameterized using experimental data from the literature and optimized using nonlinear programming (NLP) to minimize the total annualized cost (TAC), evaluating the trade-off between the number of cells and the applied current density for large-scale hydrogen production. The Results section presents the model fitting, followed by the optimal operating and design conditions obtained from the TAC minimization. Finally, the main findings and implications are summarized in the Conclusions.

## METHODS

A typical anion exchange membrane (AEM) electrolyzer cell consists of an anion exchange membrane sandwiched between an anode and a cathode, both comprising catalyst and gas diffusion layers, as well as bipolar plates containing engraved flow channels (Figure 1).

In the present system, an aqueous KOH solution is supplied to the cathode, while a mixture of $NH_3$ and KOH is fed to the anode. At the cathode, water is reduced to hydrogen and hydroxide ions via the hydrogen evolution reaction. The hydroxide ions migrate through the AEM toward the anode, where ammonia electro-oxidation produces nitrogen and water. The generated gaseous products are removed through the respective flow channels.

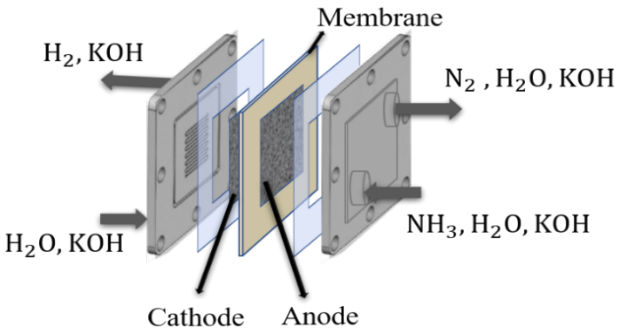


**Figure 1**. Conceptual schematic of the anion exchange membrane ammonia electrolysis cell.

### Mathematical modeling

In contrast to previously reported ammonia electrolysis models that focus either on detailed reaction mechanisms or highly resolved transport phenomena [7-8], the present work adopts a physics-based zero-dimensional modeling approach that is suitable for system-level analysis and optimization. The electrolyzer is treated as a lumped system and spatial gradients of temperature, concentration, and current density are neglected. The model formulation is based on global electrochemical relations and simplified thermal and pressure descriptions, under the following assumptions:

1. Steady-state operation at constant temperature and pressure;
2. Catalyst layers are treated as interfacial surfaces;
3. Ohmic losses are described using Ohm's law;
4. The electrolyte is an aqueous KOH solution;
5. Identical active areas and uniform current density at both electrodes;
6. Gaseous species behave as ideal gases and are uniformly distributed;
7. Uniform pressure along gas flow channels;
8. Electrolyte ohmic resistance in the electrode gap is neglected due to the zero-gap configuration;
9. Gas bubble coverage effects are not explicitly modeled, as forced electrolyte flow and the zero-gap architecture promote rapid bubble detachment.

The model builds upon established formulations previously developed for anion exchange membrane water electrolysis (AEMWE) [9–12] and alkaline water electrolysis (AWE) [13-15].

The cell voltage is calculated as the sum the reversible cell potential ($V_{rev}$) and the different overpotential contributions, namely activation ($\eta_{act}$), concentration ($\eta_{con}$), and ohmic ($\eta_{ohm}$) overpotentials, as expressed in Equation 1.

$$V_{cell} = V_{rev} + \eta_{act} + \eta_{con} + \eta_{ohm} \quad (1)$$

The reversible cell potential is calculated using the Nernst equation as expressed in Equation 2:

$$V_{rev} = V_{rev}^{0} + \frac{R \cdot T}{z \cdot F} \ln \frac{a_{H_2}^{3} \cdot a_{N_2}}{a_{NH_3}^{2}} \quad (2)$$

Where $R$ is the universal gas constant, $F$ is Faraday's constant, $a_k$ denotes the thermodynamic activity of species $k$, and $z$ is the number of electrons transferred in the overall ammonia electrolysis reaction. The standard reversible potential ($V_{rev}^{0}$) is obtained from the semi-empirical correlation proposed by Estejab et al. [16]. The thermodynamic activities of hydrogen and nitrogen are assumed to be equal to their respective partial pressures, which are calculated following the procedure described in [13].

The activity of ammonia is assumed to be equal to that of the alkaline electrolyte composed solely of KOH, since the ammonia concentration employed is relatively low. The activity of water in aqueous KOH solutions is calculated according to the correlation reported by Balej [17].

The activation overpotential is expressed as the sum of the anodic and cathodic activation contributions, derived from the Butler-Volmer formulation, and written in logarithmic form as Equation 3:

$$\eta_{act} = \frac{2.3 \cdot R \cdot T}{z \cdot \alpha_{cat} \cdot F} \log \frac{i}{i_{cat}^{0}} + \frac{2.3 \cdot R \cdot T}{z \cdot \alpha_{ano} \cdot F} \log \frac{i}{i_{ano}^{0}} \quad (3)$$

where $i$ is the operating current density, $i_{cat}^{0}$ e $i_{ano}^{0}$ are the exchange current densities at the cathode and anode, respectively, and $\alpha_{cat}$ and $\alpha_{ano}$ are the corresponding charge transfer coefficients. The exchange current densities are modeled as temperature-dependent quantities

following an Arrhenius-type relationship (Equations 4-5):

$$i_{cat}^{0} = i_{cat,ref}^{0} \cdot \exp\left[-\frac{\Delta G_{cat}}{R} \cdot \left(\frac{1}{T} - \frac{1}{T_{ref}}\right)\right] \quad (4)$$

$$i_{ano}^{0} = i_{ano,ref}^{0} \cdot \exp\left[-\frac{\Delta G_{ano}}{R} \cdot \left(\frac{1}{T} - \frac{1}{T_{ref}}\right)\right] \quad (5)$$

where $i_{cat,ref}^{0}$ and $i_{ano,ref}^{0}$ represent the exchange current densities at reference temperature $T_{ref}$, and $\Delta G_{cat}$ and $\Delta G_{ano}$ denote the activation free energies associated with the cathodic and anodic reactions, respectively.

In the present model, the charge transfer coefficients $\alpha_{cat}$ and $\alpha_{ano}$ are assumed to be temperature-dependent. Similar behavior has been reported in previous electrochemical modeling studies [9–11]. In this work, empirical correlations as functions of temperature were obtained by regression of experimental polarization data and are described by third-order polynomial expression. The nonlinear temperature dependence of $\alpha$ observed for ammonia electrolysis contrasts with the commonly assumed linear behavior in water electrolysis and reflects the higher mechanistic complexity of the ammonia oxidation reaction.

The concentration overpotential is derived from the Nernst equation combined with Fick's law to account for mass transport limitations associated with gas diffusion through the porous electrodes. Following an approach from Chang et al. [11], the concentration overpotential is expressed as Equation 6:

$$\eta_{conc} = \frac{2.3 \cdot R \cdot T}{n_{cat} \cdot F} \log \frac{C_{H_2,cat}}{C_{H_2,low}} + \frac{2.3 \cdot R \cdot T}{n_{ano} \cdot F} \log \frac{C_{N_2,ano}}{C_{N_2,low}} \quad (6)$$

where $C_{N_2,ano}$ and $C_{H_2,cat}$ are the concentrations of hydrogen and nitrogen, respectively, at the membrane–electrolyte interface, while $C_{N_2,low}$ and $C_{H_2,low}$ denote the reference concentrations at working conditions. The parameters $n_{cat} = 2$ and $n_{ano} = 6$, represent the number of electrons required to produce one mole of $H_2$ and $N_2$, respectively.

The ohmic overpotential accounts for electrodes and membrane resistances within the electrolyzer and is calculated by modeling the different cell components as electrical resistances connected in series. The effective cell resistance ($R_{cell}$) is obtained as the sum of the electrode resistances ($R_{electrodes}$), and the separator resistance, which in the present case corresponds to the anion exchange membrane ($R_{membrane}$). Accordingly, the ohmic overpotential is given by Ohm's law (Equation 7):

$$\eta_{ohm} = I \cdot R_{cell} \quad (7)$$

The total electrode resistance is calculated according to the Equation 8:

$$R_{electrodes} = \rho_{ef,cat} \cdot \frac{\delta_{cat}}{A_e} + \rho_{ef,ano} \cdot \frac{\delta_{ano}}{A_e} \quad (8)$$

where $\rho_{ef,cat}$ and $\rho_{ef,ano}$ are the effective resistivities of the cathode and anode, respectively, $\delta_{cat}$ and $\delta_{ano}$ are the corresponding electrode thicknesses, and $A_e$ is the active electrode area. The expressions used to calculate the effective resistivities are taken from the correlations reported in [13].

The membrane resistance is given by Equation 9:

$$R_m = \frac{\delta_m}{\sigma_m \cdot A_m} \quad (9)$$

where $\delta_m$ is the membrane thickness, $A_m$ is the active membrane area, and $\sigma_m$ is the ionic conductivity of the membrane material.

## Experimental data and parameter estimation

Experimental polarization data reported by Zhang et al. [1] were used to estimate the model parameters. The experiments were conducted in a zero-gap membrane electrode assembly (MEA) electrolyzer with an active area of 5 $cm^2$, operating between 323 and 363 K. The anode was supplied with an aqueous solution containing 3 M KOH and 3 M $NH_3$, while the cathode was fed with 3 M KOH, both at a flow rate of 3 mL/min and atmospheric pressure.

Model parameters, including anodic and cathodic exchange current densities, activation energies, and membrane thickness, were estimated through nonlinear least-squares regression. Parameter estimation was performed using a routine developed in Python (Python Software Foundation, USA), employing the curve_fit function from the SciPy library together with NumPy [18]. The optimization was carried out using the Trust-Region Reflective algorithm.

## Model performance metrics

Model performance was evaluated by calculating the determination coefficient ($R^2$), mean absolute error (MAE), mean absolute percentage error (MAPE), and root mean square error (RMSE). Parameter uncertainty and identifiability was assessed using the bootstrap method, confirming the robustness of the estimated parameters.

## Optimization framework

To evaluate the techno-economic performance of the zero-gap ammonia electrolyzer and its scale-up to plant level, the developed electrochemical model was embedded into a nonlinear optimization framework to minimize the total annual cost (TAC), implemented in Python using the Pyomo package (version 6.10.0) [19]. The formulation accounts for electrochemical, thermal, and economic trade-offs, enabling the identification of optimal operating and design conditions.

The TAC (Equation 10) accounts for both capital and operating expenditures associated with the electrolyzer system.

Capital expenditure (CAPEX, Equation 11) was assumed to be proportional to the number of cells (N), the cost of a cell per area ($C_{cell}$), and the cell area ($A_{cell}$).

Operating expenditure (OPEX, Equation 12) includes

electricity and steam consumption. The capital recovery factor (CRF, Equation 13) was calculated assuming a plant lifetime ($n$) of 20 years and interest rate ($j$) of 10%. The parameters used to calculate the expenditures are list in Table 1.

$$\mathrm{TAC} = \mathrm{CRF} \bullet \mathrm{CAPEX} + \mathrm{OPEX} \quad (10)$$

$$\mathrm{CAPEX} = \mathrm{N} \bullet \mathrm{C_{cell}} \bullet \mathrm{A_{cell}} \quad (11)$$

$$\mathrm{OPEX} = \mathrm{C_{elect}} \bullet \mathrm{P} \bullet \mathrm{h_{op}} + \mathrm{C_{steam}} \bullet \mathrm{Q_t} \bullet \mathrm{h_{op}} \quad (12)$$

$$\mathrm{CRF} = \frac{\mathrm{j(1+j)^n}}{\mathrm{(1+j)^n - 1}} \quad (13)$$

where $C_{elect}$ is the electricity cost (USD/MWh), $P$ is the total electrical power (MW), $h_{op}$ is the annual operating time (h/year), $C_{steam}$ is the steam cost (USD/GJ) and $Q_t$ is the total thermal demand (GJ).

The thermal energy required to heat the electrolyte was estimated using a surrogate model derived from process simulations performed in Aspen Plus v.12, using a temperature-dependent polynomial correlation. These simulations were used to calculate the specific heat requirement per unit mass of electrolyte solution, $Q_{spec}$(GJ/kg), under representative operating conditions.

Within the optimization framework, the total thermal demand was then obtained by scaling the specific heat requirement with the electrolyte mass flow per cell and the total number of cells, Equation 14:

$$Q_t = Q_{spec} \bullet \dot{m}_{sol} \bullet N \quad (14)$$

where $\dot{m}_{sol}$ is the electrolyte mass flow rate per cell.

**Table 1.** Main parameters of the optimization problem.

| Parameter | Value | Reference |
|---|---|---|
| $\mathrm{h_{op}}$ (h/year) | 8000 | Adopted |
| $\mathrm{C_{cell}}$ (USD/m$^2$) | 16200 | [20] |
| $\mathrm{C_{steam}}$ (USD/GJ) | 12.85 | [21] |
| $\mathrm{C_{elect}}$ (USD/MWh) | 136.95 | [21] |
| $\mathrm{A_{cell}}$ (m$^2$) | 3.14 | [1] |

The main decision variables of the optimization problem are:

- Current density, $i$ (A/cm$^2$);
- Number of cells, N;
- Operating temperature, T (K).

These variables simultaneously control the electrochemical performance of the cell and the overall plant sizing, directly affecting hydrogen production, energy consumption, and total system cost.

The optimization problem was formulated as the minimization of TAC, subject to electrochemical, physical, thermal, operational, and hydrogen production constraints, as expressed in Equations 15-20.

$$\min \mathrm{TAC}, (\mathrm{Equation\ 10}) \quad (15)$$

$$\mathrm{s.t.\ cell\ voltage\ equation}, Eq.(1) \quad (16)$$

$$\mathrm{H_2\ production}: \frac{\mathrm{I}}{2 \bullet \mathrm{F}} MM_{H_2} \geq 1250\ \mathrm{kg/h} \quad (17)$$

$$\mathrm{T^l} \leq \mathrm{T} \leq \mathrm{T^u} \quad (18)$$

$$\mathrm{N^l} \leq \mathrm{N} \leq \mathrm{N^u} \quad (19)$$

$$\mathrm{i^l} \leq \mathrm{i} \leq \mathrm{i^u} \quad (20)$$

where T is the operating temperature of the electrochemical cell, which was allowed to vary between $\mathrm{T^l}$=323 K and $\mathrm{T^u}$=353 K. The current density $i$ was evaluated in the range $\mathrm{i^l}$=0 to $\mathrm{i^u}$=2 A/cm$^2$, and the number of electrochemical cells was varied between $\mathrm{N^l}$=0 and $\mathrm{N^u}$=400 000.

A minimum hydrogen production target of 1250 kg/h was imposed to represent large-scale centralized production, consistent with the hydrogen demand of multiple refueling stations, where a single station typically consumes about 1000 kg/day of hydrogen.

The resulting nonlinear programming (NLP) problem was solved using the IPOPT solver [22], which is well suited for constrained nonlinear optimization with continuous decision variables.

## RESULTS

### Modeling results

The model parameters were estimated through nonlinear regression using the experimental polarization data. The regressed model was then compared with the experimental measurements to assess its ability to reproduce the observed electrochemical behavior.

Figure 2 presents the experimental polarization curves together with the corresponding model predictions at different operating temperatures between 323 and 353 K. Over this temperature range, the model reproduces the experimental cell voltages with good agreement across the investigated current density domain. At higher temperatures beyond the analyzed range, deviations are expected due to the reduced ammonia solubility at elevated temperatures, which affects mass transport phenomena.

Statistical goodness-of-fit indicators as $R^2$= 0.9874, and MAE=0.0126, MAPE= 2.72%, and RMSE = 0.0155, indicate a strong agreement between the regressed model and the experimental data within the range of operating

conditions considered.

The estimated parameters are reported in Table 2. The obtained values for the exchange current densities at reference temperature, fall within ranges commonly reported in the literature for alkaline electrolysis [9], [13], [23], varying between $10^{-3}$ and $10^{-11}$ A/cm$^2$, supporting the physical consistency of the proposed modeling approach. Similarly, the estimated activation free energies are close to values previously reported in the literature [23], [24].

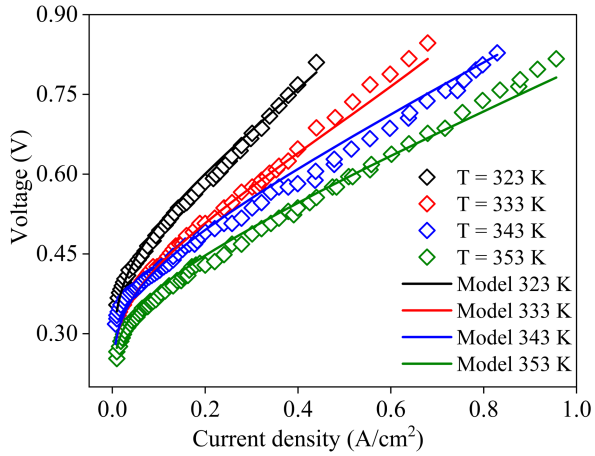


**Figure 2**. Comparison of experimental data with model predictions.

**Table 2.** Estimated model parameters from non-linear regression.

| Parameters | Value |
|---|---|
| $i^0_{ano,ref}$ (A/cm$^2$) | $7.64 \cdot 10^{-7}$ |
| $\Delta G_{ano}$ (J/mol) | 24935.61 |
| $i^0_{cat,ref}$ (A/cm$^2$) | $3.32 \cdot 10^{-5}$ |
| $\Delta G_{cat}$ (J/mol) | 16524.13 |
| $\delta_m$ (cm) | 0.0034 |

## Optimization results

Solving the nonlinear optimization problem resulted in a unique set of operating and design conditions that minimize TAC while satisfying the minimum hydrogen production constraint. Figure 3 illustrates the variation of TAC with current density for the different operating temperatures considered. A well-defined minimum is observed at 353 K, indicating that this temperature provides the most favorable trade-off between improved electrochemical performance and increased thermal and operating costs.

At the optimal temperature of 353 K, the optimal current density was found to be 0.82 A/cm$^2$. This value represents a compromise between higher hydrogen production rates and the increase in activation, concentration, and ohmic overpotentials at elevated current densities. The resulting optimal cell voltage is approximately 0.81 V, leading to a total plant electrical power consumption of about 27.1 MW. The optimal current density and cell voltage obtained in this work are in good agreement with limits reported for ammonia electrolysis, which indicate that economically viable operation requires current densities close to 1 A/cm$^2$ while maintaining the applied cell potential below approximately 1 V [25].

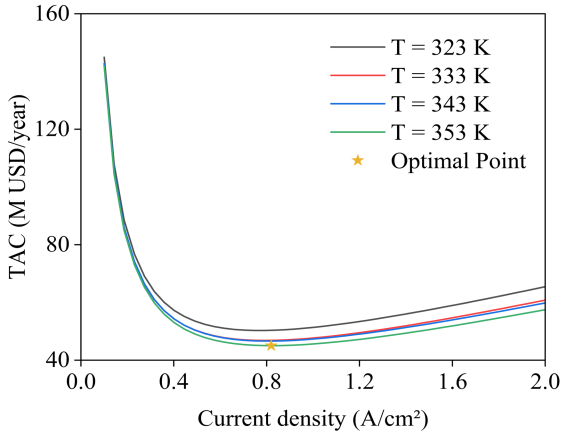


**Figure 3**. Variation of TAC at different temperatures.

The corresponding optimal number of cells was determined to be $N$ = 1302, as illustrated in Figure 4 at 353 K.

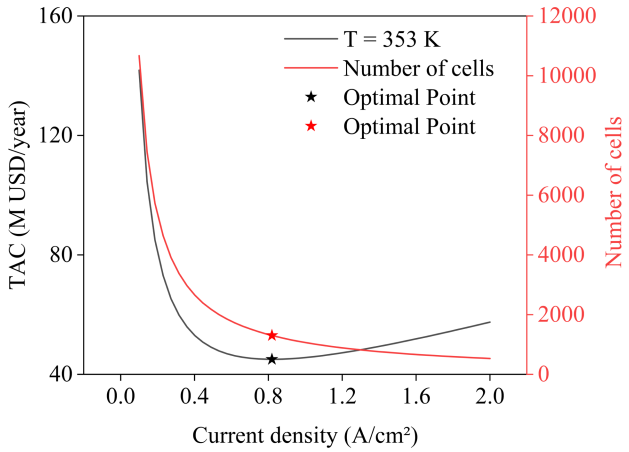


**Figure 4**. Optimization of TAC and number of cells at 353 K.

The estimated capital expenditure (CAPEX) under optimal conditions amounts to approximately 132.5 million USD, dominated by the installed electrochemical active area. The annual operating expenditure (OPEX) was calculated as approximately 29.5 million USD/year, primarily driven by electricity and steam consumption. The resulting minimum TAC is approximately 45.0 million

USD/year. Under these optimal conditions, the system achieves the target hydrogen production rate of 1250 kg/h. The estimated cost of hydrogen production is approximately 4.5 USD/kg $H_2$, excluding ammonia feedstock cost, and it falls within the range reported values for alkaline water electrolysis [26]. A complete techno-economic assessment including ammonia supply, storage, logistics, and sensitivity analysis is left for future work.

## CONCLUSIONS

This work developed a mathematical model of a zero-gap AEM ammonia electrolyzer integrated into a techno-economic optimization framework. The model was fitted to experimental polarization data and describes the main factors affecting cell voltage, energy efficiency, and hydrogen production, showing good agreement ($R^2$ = 0.9874). For the base case, optimal configuration corresponds to a temperature of 353 K, a current density of 0.82 A/cm$^2$, and 1302 cells, resulting in a TAC of about 45.0 MUSD/year.

## ACKNOWLEDGEMENTS

The authors gratefully acknowledge Petronas and the São Paulo Research Foundation (FAPESP) (#2020/15230-5 and #2024/08858-9) for their financial support, ANP (Brazilian National Oil, Natural Gas, and Biofuels Agency) for the strategic importance of its support under the R&D levy regulation, and the Research Center for Greenhouse Gas Innovation (RCGI). The authors also thank the National Council for Scientific and Technological Development (CNPq) (#304346/2025-0). This study was financed in part by the Personnel Coordination for the Improvement of HigherLevel Personnel-Brazil (CAPES)-Finance Code 001.

## AUTHOR IDENTIFIERS

Lefrán LEH: 0009-0006-9712-3454
Avilez LAC: 0000-0001-8320-863X
Bresciani AE: not available
Oller CAO: 0000-0001-6110-0249
Alves RMB: 0000-0002-1914-5133

## REFERENCES

1. Zhang K, Han Y, Zhao Y, Wei T, Fu J, Ren Z, Xu X, Zhou L, Shao Z. Energy-efficient and cost-effective ammonia electrolysis for converting ammonia to green hydrogen. Cell Reports Physical Science 5:102171 (2024). https://doi.org/10.1016/j.xcrp.2024.102171
2. Mansilla C, Bourasseau C, Cany C, Guinot B, Le Duigou A, Lucchese P. Hydrogen applications: overview of the key economic issues and perspectives. Hydrogen Supply Chains :271-292 (2018). https://doi.org/10.1016/b978-0-12-811197-0.00007-5
3. Niaz S, Manzoor T, Pandith AH. Hydrogen storage: materials, methods and perspectives. Renewable and Sustainable Energy Reviews 50:457-469 (2015). https://doi.org/10.1016/j.rser.2015.05.011
4. Lucentini I, Garcia X, Vendrell X, Llorca J. Review of the decomposition of ammonia to generate hydrogen. Ind. Eng. Chem. Res. 60:18560-18611 (2021). https://doi.org/10.1021/acs.iecr.1c00843
5. Baeck J. S-injective modules. Rev. Real Acad. Cienc. Exactas Fis. Nat. Ser. A-Mat. 118: (2023). https://doi.org/10.1007/s13398-023-01514-7
6. Serrano-Jiménez J, Martín C, Pinzón M, Sánchez P, de la Osa AR. Exploring the potential of ammonia electrolysis for hydrogen production: from lab-performance to stack architectures. Current Opinion in Chemical Engineering 51:101204 (2026). https://doi.org/10.1016/j.coche.2025.101204
7. Estejab A, Daramola DA, Botte GG. Mathematical model of a parallel plate ammonia electrolyzer for combined wastewater remediation and hydrogen production. Water Research 77:133-145 (2015). https://doi.org/10.1016/j.watres.2015.03.013
8. Diaz LA, Botte GG. Mathematical modeling of ammonia electrooxidation kinetics in a polycrystalline pt rotating disk electrode. Electrochimica Acta 179:519-528 (2015). https://doi.org/10.1016/j.electacta.2014.12.162
9. Gunuru M, Paravada M. Mathematical modeling of an AEMWE: investigating optimum operating conditions of an alkaline-fed AEM electrolyzer. International Journal of Hydrogen Energy 157:150320 (2025). https://doi.org/10.1016/j.ijhydene.2025.150320
10. Gomez Vidales A, Millan NC, Bock C. Modeling of anion exchange membrane water electrolyzers: the influence of operating parameters. Chemical Engineering Research and Design 194:636-648 (2023). https://doi.org/10.1016/j.cherd.2023.05.004
11. Chang SC, Gu RE, Chan YH. Parameter analysis of anion exchange membrane water electrolysis system by numerical simulation. Energies 17:5682 (2024). https://doi.org/10.3390/en17225682
12. D. Lee, M. Kim, and I. Moon, *Mathematical Modeling of Anion Exchange Membrane Water Electrolyzer*, vol. 52. Elsevier Masson SAS, 2023.
13. Abdin Z, Webb CJ, Gray EM. Modelling and simulation of an alkaline electrolyser cell. Energy 138:316-331 (2017). https://doi.org/10.1016/j.energy.2017.07.053
14. Hu S, Guo B, Ding S, Yang F, Dang J, Liu B, Gu J,

Ma J, Ouyang M. A comprehensive review of alkaline water electrolysis mathematical modeling. Applied Energy 327:120099 (2022). https://doi.org/10.1016/j.apenergy.2022.120099
15. Garibaldi L, Blanco-Aguilera R, Berasategi J, Martinez-Agirre M, Giorgi G, Bracco G, Penalba M. Holistic and dynamic mathematical model for the assessment of offshore green hydrogen generation and electrolyser design optimisation. Energy Conversion and Management 294:117488 (2023). https://doi.org/10.1016/j.enconman.2023.117488
16. Estejab A, Daramola DA, Botte GG. A semi-empirical model of ammonia electrolysis in comparison to water electrolysis. Meet. Abstr. MA2012-02:108-108 (2012). https://doi.org/10.1149/ma2012-02/2/108
17. BALEJ J. Water vapour partial pressures and water activities in potassium and sodium hydroxide solutions over wide concentration and temperature ranges. International Journal of Hydrogen Energy 10:233-243 (1985). https://doi.org/10.1016/0360-3199(85)90093-x
18. P. Virtanen *et al.*, "SciPy 1.0: fundamental algorithms for scientific computing in Python, " *Nat. Methods*, vol. 17, no. 3, pp. 261–272, Mar. 2020.
19. Bynum ML, Hackebeil GA, Hart WE, Laird CD, Nicholson BL, Siirola JD, Watson JP, Woodruff DL. Pyomo overview. Springer Optimization and Its Applications :25-36 (2021). https://doi.org/10.1007/978-3-030-68928-5_3
20. Le Bideau D, Chocron O, Mandin P, Kiener P, Benbouzid M, Sellier M, Kim M, Ganci F, Inguanta R. Evolutionary design optimization of an alkaline water electrolysis cell for hydrogen production. Applied Sciences 10:8425 (2020). https://doi.org/10.3390/app10238425
21. Eurostat, "Electricity and natural gas price statistics., " *Stat. Explain. 2025*.
22. Wächter A, Biegler LT. On the implementation of an interior-point filter line-search algorithm for large-scale nonlinear programming. Math. Program. 106:25-57 (2005). https://doi.org/10.1007/s10107-004-0559-y
23. Rodríguez J, Amores E. CFD modeling and experimental validation of an alkaline water electrolysis cell for hydrogen production. Processes 8:1634 (2020). https://doi.org/10.3390/pr8121634
24. Gwak J, Choun M, Lee J. Alkaline ammonia electrolysis on electrodeposited platinum for controllable hydrogen production. ChemSusChem 9:403-408 (2015). https://doi.org/10.1002/cssc.201501046
25. Long H, Sit CY, Paliwal A, Cheng T, Gupta JK, Reynolds MA, Son YJ, Zhang K, Gewirth AA, Kenis PJA. Alkaline ammonia electrolysis in a membrane electrode assembly cell: parameter optimization and dynamic operation. EES Catal. 4:465-482 (2026). https://doi.org/10.1039/d5ey00324e
26. M. R. Cerqueda, "Selección natural en el hidrógeno verde : Solo quedarán los mejores Autor, " 2024.